Oxidation of Metals, Vol. 5, No. 3, 1972

The Contribution of Different Types of Point Defects to Diffusion in CoO and NiO During Oxidation of the Metals*

G. J. Koel†‡ and P. J. Gellings†

Received October 9, 1972

Starting from a general model for the defect structure of nickel and cobalt oxides, the concentrations and diffusion coefficients of the major defects in these oxides are determined as functions of temperature and oxygen pressure. At the higher oxygen pressures, the majority of cation defects are mono-negative metal ion vacancies while at lower oxygen pressures appreciable concentrations of dinegative metal ion vacancies are present. It is shown that it is highly probable that the anion defects are dipositive oxygen vacancies. However, these are minority defects over the whole stability range of the oxides. It is not possible with the methods discussed here to determine their individual concentrations and diffusion coefficients. On the basis of this defect structure, a model for the oxidation of Co and Ni is proposed; the deductions from this model are compared with experimental results and good agreement is observed. It is shown that more than one type of defect contributes to the total transport through the oxide. For cobalt, these are mono- and dinegative metal ion vacancies; for nickel, dipositive oxygen vacancies also make a significant contribution.

INTRODUCTION

Since the pioneering work of Wagner,[1,2] the parabolic rate equation for the high temperature oxidation of metals is explained by assuming that volume diffusion of metal or oxygen ions is the rate-determining step. Kröger[3] has shown that there is a direct connection between the defect structure of the oxide and the parabolic rate equation.

*This work is part of a thesis submitted by G. J. Koel to the Twente University of Technology.

†Laboratory for Inorganic Chemistry and Inorganic Materials Science, Department of Chemical Engineering, Twente University of Technology, Enschede, Netherlands.

‡Present address: Philips Research Laboratories, Eindhoven, Netherlands.

In most applications of this theory it has been assumed that the concentration of only one type of defect (with charge compensation by electrons or electron holes) determines the oxidation process. This assumption, however, cannot be true in general, because the defect concentrations all depend upon oxygen pressure in different ways. As this pressure is much higher at the gas–oxide interface (0.1–1 atm) than at the oxide–metal interface (equal to the dissociation pressure of the oxide, often $<10^{-10}$ atm), the defect concentrations must show large relative shifts.

In this paper the defect model for NiO and CoO and the diffusion of defects will first be described briefly. This will then be applied to a kinetic model for the oxidation of the metals and the results will be discussed.

Two basic assumptions will be made throughout: (1) the oxidation rate is much lower than the rates of creation and annihilation of defects so that the defects are in equilibrium everywhere in the oxide layer; (2) the diffusion coefficients of the defects are independent of their concentration.

THE DEFECT STRUCTURE OF CoO AND NiO

For the model of the oxidation mechanism the following defect equilibria have to be considered

$$\tfrac{1}{2}O_2 \rightleftarrows V_M^x + O_O \qquad K_a = [V_M^x]p_{O_2}^{-1/2} \tag{1}$$

$$V_M^x \rightleftarrows V_M' + h^{\cdot} \qquad K_b = [V_M'][h^{\cdot}][V_M^x]^{-1} \tag{2}$$

$$V_M' \rightleftarrows V_M'' + h^{\cdot} \qquad K_c = [V_M''][h^{\cdot}][V_M']^{-1} \tag{3}$$

$$0 \rightleftarrows V_M'' + V_O^{\cdot\cdot} \qquad K_s = [V_M''][V_O^{\cdot\cdot}] \tag{4}$$

$$0 \rightleftarrows e' + h^{\cdot} \qquad K_i = [e'][h^{\cdot}] \tag{5}$$

Mole fractions are used throughout and the defect notation of Kröger[3] (see also Van Gool[4]) is followed.

As is usually assumed and as has been shown by us* e' and $V_O^{\cdot\cdot}$ are minority defects over the whole existence ranges of CoO and NiO. Thus the electroneutrality condition can be written as

$$[V_M'] + 2[V_M''] = [h^{\cdot}] \tag{6}$$

From Eqs. (1) to (3) together with (6) it follows that

$$[h^{\cdot}]^3 = K_aK_b(2K_c + [h^{\cdot}])p_{O_2}^{1/2} \tag{7}$$

Measurement of $[h^{\cdot}]$ as a function of oxygen pressure thus makes it possible to calculate K_aK_b and K_c.

*See the footnote on page 187.

Experimental Results*

The defect structures of CoO and NiO have been determined quantitatively by thermogravimetry and electrical conductivity measurements at from 950 to 1350°C and at oxygen pressures ranging from 1 atm to the dissociation pressures of the oxides. For CoO it has been established that over the whole stability range the neutral vacancy V_M^x is a minority defect. This is in agreement with the results of Eror and Wagner[5] but not with those of Fischer and Tannhauser.[6] For NiO it has been found that at oxygen pressures above 10^{-3} atm the defect concentrations as determined by thermogravimetry and electrical conductivity techniques are approximately proportional to $p_{O_2}^{1/4}$. This means that at these pressures V'_M is the majority defect. Meyer and Rapp,[7] however, are of the opinion that V''_M is the majority defect in NiO and that the $p_{O_2}^{1/4}$ dependence is caused by the presence of supravalent impurities. In a later publication we hope to show that these impurities, if they are present, associate partly with the cation vacancies and therefore can hardly influence the other defect concentrations through the electroneutrality condition. Furthermore, throughout the work we used spectrographically pure Ni (Johnson-Matthey) for oxidation to NiO. The amount of trivalent impurities present after the measurements was in all cases lower than 100 ppm.

From the experimental results it follows that for CoO

$$\begin{aligned} K_a K_b &= 2.17 \times 10^{-2} \times \exp(-15{,}600/RT) \\ K_c &= 0.17 \times \exp(-18{,}500/RT) \end{aligned} \tag{8}$$

In Fig. 1 the dependence of the concentrations of the majority defects upon oxygen pressure at 1146°C as calculated from Eqs. (1), (2), and (3) using (8) is shown. At other temperatures similar curves were obtained.

For NiO it is found from the experimental results that

$$\begin{aligned} K_a K_b &= 4 \times 10^{-2} \times \exp(-40{,}000/RT) \\ K_c &= 0.17 \times \exp(-25{,}000/RT) \end{aligned} \tag{9}$$

Figure 2 shows the defect concentrations in NiO at 1150°C as calculated from Eqs. (1), (2), and (3) using Eq. (9) as a function of oxygen pressure.

Both Figs. 1 and 2 show that at oxygen pressures near 1 atm V'_M is the majority defect and that at sufficiently low oxygen pressure V''_M becomes the majority defect. The absolute values of $[V_O^{\cdot\cdot}]$ and $[e']$ cannot be determined and it is only possible to conclude from Eqs. (4) and (5) that $[V_O^{\cdot\cdot}] \sim [V''_M]^{-1}$ and $[e'] \sim [h^{\cdot}]^{-1}$.

*This work will be described more extensively in a publication which is in preparation.

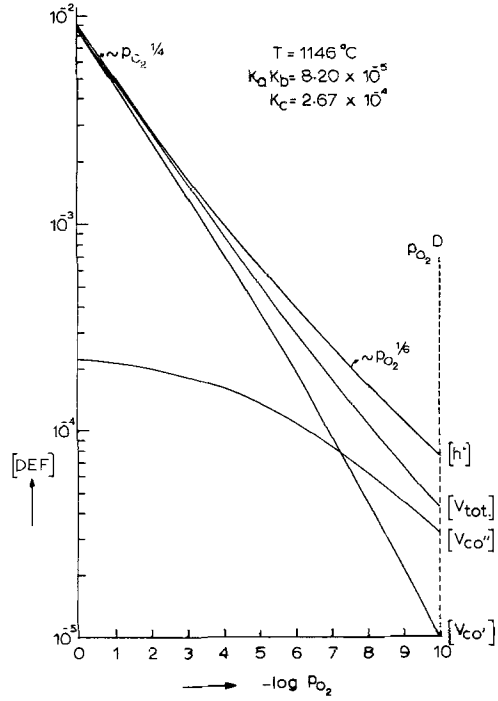

Fig. 1. Defect concentrations in CoO at 1146°C.

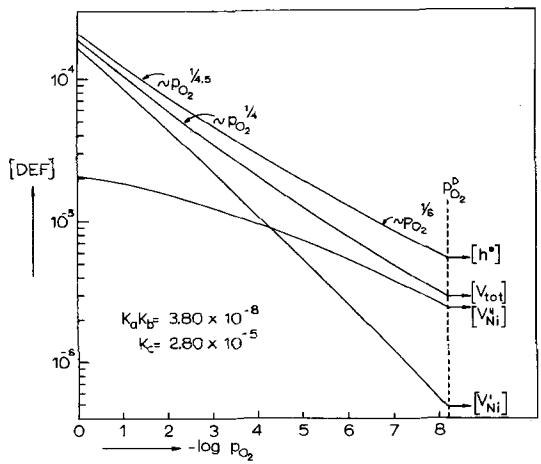

Fig. 2. Defect concentrations in NiO at 1150°C.

THE DIFFUSION OF DEFECTS IN CoO AND NiO

Cation Defects

From the results of the preceding section it follows that in NiO and CoO at oxygen pressures above 10^{-4} atm the electroneutrality condition can be approximated by

$$[V'_M] = [h^{\cdot}] \tag{10}$$

and equilibrium with the gas phase by

$$\tfrac{1}{2}O_2 \rightleftarrows V'_M + h^{\cdot} + O_O \tag{11}$$

At lower oxygen pressures the cation vacancies dissociate according to Eq. (3) and when this dissociation is complete the electroneutrality condition becomes

$$2[V''_M] = [h^{\cdot}] \tag{12}$$

However, as Figs. 1 and 2 show, complete dissociation is not reached in these oxides.

If an oxide is in equilibrium with oxygen at pressure $p^0_{O_2}$, and then the pressure is suddenly changed from $p^0_{O_2}$ to $p^I_{O_2}$ at $t = 0$, a defect current flows. Depending upon the approximation used in the electroneutrality condition, Eq. (10) or (12), these defect currents are mainly due to either $V'_M + h^{\cdot}$ or to $V''_M + 2h^{\cdot}$.

The diffusion coefficients of the cation vacancies can now be determined using either thermogravimetry of electrical conductivity measurement by determining the change in weight or resistance as a function of time after changing the oxygen pressure.

Solutions of Fick's second law for samples with dimensions $a \times b \times d$ cm^3 and $d \ll a, b$ have been given by Jost[8] and Crank.[9] From these solutions it can be deduced that for the thermogravimetric determination we have

$$\ln(w_\infty - w_t) = \frac{-\pi^2(n+1)D_{V_M^{n'}} \times t}{d^2} + \text{constant} \tag{13}$$

Here, $(w_\infty - w_t)$ is the weight difference at time t when equilibrium reestablishes itself; n is the effective vacancy charge (1 or 2); $D_{V_M^{n'}}$ is the diffusion coefficient of $V_M^{n'}$.

For the conductivity measurements we have similarly

$$\ln(\sigma_\infty - \sigma_t) = \frac{-\pi^2(n+1)D_{V_M^{n'}} \times t}{d^2} + \text{constant} \tag{14}$$

where $(\sigma_\infty - \sigma_t)$ is the difference in conductivity at time t when a new equilibrium is reached.

By plotting $\ln(w_\infty - w_t)$ and $\ln(\sigma_\infty - \sigma_t)$ against time, the quantity $(n+1)D_{V_M''}$ and hence $D_{V_M''}$ can be determined from the slope of the resulting straight line.

Experimental Results

Using thermogravimetry at oxygen pressures from 10^{-3} to 1 atm and temperatures between 950 and 1350°C we found

$$D_{V_{Co}''} = 8.3 \times 10^{-3} \times \exp(-24{,}000/RT)\,\text{cm}^2\,\text{sec}^{-1} \tag{15}$$

From the conductivity measurements it was found that

$$D_{V_{Co}''} = 2 \times 10^{-2} \times \exp(-26{,}000/RT)\,\text{cm}^2\,\text{sec}^{-1} \tag{16}$$

There is thus a reasonable agreement between the values of $D_{V_{Co}''}$ as determined by these two methods.

Measurements were also performed at oxygen pressures close to the dissociation pressure of CoO. Assuming that in this region diffusion is mainly due to V_{Co}'', it could be shown that $D_{V_{Co}''} \approx D_{V_{Co}''}$.

From the conductivity measurements it was found that going from $p_{O_2}^0 = 10^{-3}$ to $p_{O_2}^I = 10^{-2}$ atm on the one hand and from $p_{O_2}^0 = 10^{-2}$ to $p_{O_2}^I = 1$ atm on the other hand, gave a significant increase (approximately 20%) in $D_{V_{Co}''}$ [Eq. (16) gives the average of the measurements at different values of p_{O_2}]. This was probably owing to increasing interaction between the vacancies. The accuracy of the thermogravimetric method was too low to determine this oxygen pressure dependence.

The much smaller defect concentrations in NiO made it impossible to determine $D_{V_{Ni}''}$ by thermogravimetry. From conductivity measurements at oxygen pressures above 10^{-3} atm and at temperatures between 975 and 1350°C we found

$$D_{V_{Ni}''} = 2.2 \times 10^{-3} \times \exp(-24{,}600/RT)\,\text{cm}^2\,\text{sec}^{-1} \tag{17}$$

At oxygen pressures below 10^{-3} atm, reproducible results were not obtained because at these low conductivities effects of static electricity and induced currents from the furnace winding cause too large a loss of accuracy. However, on the basis of the results obtained for CoO it is reasonable to suppose that in NiO we will also find $D_{V_{Ni}''} \approx D_{V_{Ni}''}$.

The diffusion coefficients found in this investigation are about 2 to 4 times larger than those found by Price and Wagner.[10] The calculated value of the tracer diffusion coefficient of Co in CoO using the defect concentrations from pages 186–188 agrees well with the experimentally determined values of Cheng *et al.*[11] and of Carter and Richardson.[12]

The Diffusion of Oxygen Defects

Chen and Jackson[13] have tried to determine oxygen diffusion coefficients in CoO as a function of p_{O_2} using an ^{18}O technique but were unable to obtain reproducible results. Neither do other authors[14,15] give oxygen diffusion coefficients as a function of p_{O_2}. Chen and Jackson[13] did determine D_O^T at 1429°C and $p_{O_2} = 0.21$ atm in CoO with additions of known amounts of Li_2O and Al_2O_3. Their results are given in Fig. 3. Using the defect equilibria discussed on pages 186–188, it can be deduced that

$$[h^{\cdot}]^2([h^{\cdot}] + [Al'_{Co}]) = K_a K_b (2K_c + [h^{\cdot}]) p_{O_2}^{1/2} \tag{18}$$

$$[h^{\cdot}]^2([h^{\cdot}] - [Li'_{Co}]) = K_a K_b (2K_c + [h^{\cdot}]) p_{O_2}^{1/2} \tag{19}$$

With the values of $K_a K_b$ and K_c from Eq. (8) $[h^{\cdot}]$ can be calculated as a function of $[Al'_{Co}]$ and $[Li'_{Co}]$ at $p_{O_2} = 0.21$ atm. From the defect equilibria we can also deduce that $[V_O^{\cdot}] \sim [h^{\cdot}]$ and $[V_O^{\cdot\cdot}] \sim [h^{\cdot}]^2$. Furthermore, $D_O^T = f \times D_{V_O^n} \cdot [V_O^n]$ where f is a correlation factor and $D_{V_O^n}$ is the diffusion coefficient of an oxygen vacancy with effective charge $n+$. Thus $D_O^T \sim [h^{\cdot}]$ if diffusion is determined by monopositive oxygen vacancies and $D_O^T \sim [h^{\cdot}]^2$ if it is determined by dipositive oxygen vacancies. In Fig. 3 the curves $[h^{\cdot}]/[h^{\cdot}]_0$ and $[h^{\cdot}]^2/[h^{\cdot}]_0^2$ are also drawn as a function of the concentrations $[Al'_{Co}]$ and $[Li'_{Co}]$ where $[h^{\cdot}]_0$ is the hole concentration in the pure oxide. $D_O^T \sim [h^{\cdot}]^2$ agrees much better with the experimental results than $D_O^T \sim [h^{\cdot}]$ and we conclude that oxygen diffusion occurs via $V_O^{\cdot\cdot}$. If we make the plausible assumption that $D_{V_O^{\cdot}} \approx D_{V_O^{\cdot\cdot}}$ this also means that $[V_O^{\cdot\cdot}] \gg [V_O^{\cdot}]$ at $p_{O_2} = 0.21$ atm. Chen and Jackson[13] assumed that oxygen diffusion occurred via

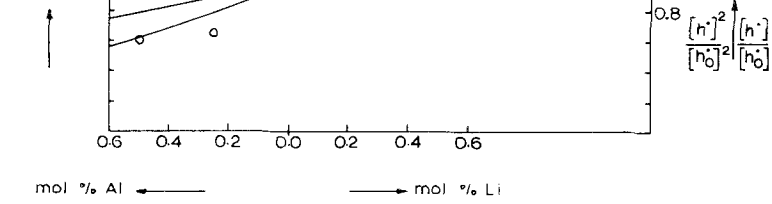

Fig. 3. D_O^T in CoO with varying Al_2O_3 and Li_2O concentration compared with $[h^{\cdot}]/[h^{\cdot}]_0$ and $[h^{\cdot}]^2/[h^{\cdot}]_0^2$. O, Experimental results of Chen and Jackson[13] at $T = 1429$°C.

$V_O^{\cdot}$ and these authors subsequently adjusted $K_a K_b p_{O_2}^{1/2}$ so that $D_O^T \sim [h^{\cdot}]$. In this way they found $K_a K_b p_{O_2}^{1/2} = 3.6 \times 10^{-5}$ at 1429°C and $p_{O_2} = 0.21$ atm. This does not agree, however, with our work where $K_a K_b p_{O_2}^{1/2} = 10^{-4}$ under these circumstances.

From the results of Chen and Jackson it follows that for pure CoO:

$$D_O^T(\text{CoO}) = 50 \times \exp(-95{,}000/RT)\,\text{cm}^2\,\text{sec}^{-1} \tag{20}$$

at $p_{O_2} = 0.21$ atm. Similarly O'Keeffe and Moore[16] found for pure NiO:

$$D_O^T(\text{NiO}) = 6.2 \times 10^{-4} \times \exp(-57{,}500/RT)\,\text{cm}^2\,\text{sec}^{-1} \tag{21}$$

at $p_{O_2} = 0.065$ atm. These authors also observed that D_O^T increased with increasing oxygen pressure, which points to oxygen diffusion via interstitial ions. As no data are given either for the magnitude of this increase or for the blank determinations, which are very important for the measurements of D_O^T, it is not clear how significant the increase is.

From the sizes of the oxygen ions, 2.70 Å diameter, and of the interstitial holes in NiO, 0.85 Å diameter, it seems improbable that interstitial oxygen ions can be present in a sufficiently high concentration to be responsible for oxygen diffusion. It is much more likely that, just as in CoO, oxygen diffusion occurs via oxygen vacancies, as is corroborated by the experiments of Reynen.[17]

To test if oxygen diffusion via vacancies can account for the values found by O'Keeffe and Moore for D_O^T(NiO), this quantity may be calculated from D_O^T(CoO). Because of the great structural similarity between CoO and NiO, it is reasonable to suppose that $D_{V_O^{\cdot\cdot}}(\text{NiO}) \approx D_{V_O^{\cdot\cdot}}(\text{CoO})$ so that we find:

$$\begin{aligned} D_O^T(\text{NiO})/D_O^T(\text{CoO}) &\approx [V_O^{\cdot\cdot}](\text{NiO})/[V_O^{\cdot\cdot}](\text{CoO}) = K_s(\text{NiO})/K_s(\text{CoO}) \\ &\quad \times [V''_{Co}]/[V''_{Ni}] \approx [V''_{Co}]/[V''_{Ni}] \end{aligned} \tag{22}$$

where, again on account of the similarity between CoO and NiO, it has been assumed that $K_s(\text{NiO}) \approx K_s(\text{CoO})$. At oxygen pressures $> 10^{-3}$ atm we have as a good approximation that $[V''_M] = K_c$ and thus

$$\begin{aligned} D_O^T(\text{NiO})/D_O^T(\text{CoO}) &\approx K_c(\text{CoO})/K_c(\text{NiO}) \\ &= \exp(-6500/RT)\,\text{cm}^2\,\text{sec}^{-1} \end{aligned} \tag{23a}$$

Combining (23a) and (21) gives

$$D_O^T(\text{NiO}) \approx 50 \times \exp(-88{,}500/RT)\,\text{cm}^2\,\text{sec}^{-1} \tag{23b}$$

at $p_{O_2} = 0.21$ atm. As both $[V_O^{\cdot\cdot}]$ and $[V''_M]$ are only slightly dependent upon

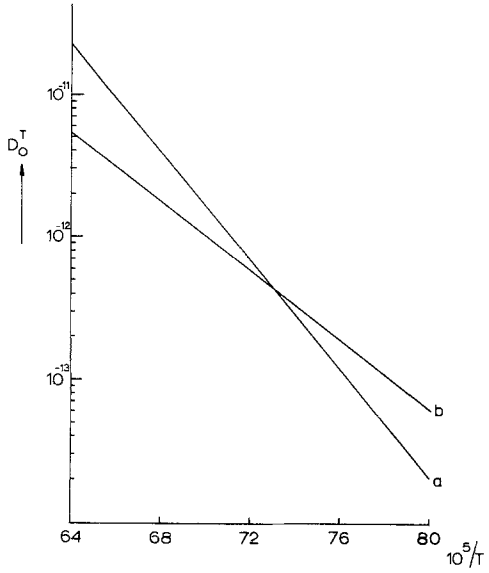

Fig. 4. Tracer diffusion coefficients of oxygen in NiO. a, Calculated from Ref. 13; b, results of Ref. 16.

p_{O_2} at oxygen pressures $>10^{-3}$ atm, we have

$$D_O^T(\text{NiO})_{p_{O_2}=0.21\,\text{atm}} \approx D_O^T(\text{NiO})_{p_{O_2}=0.065\,\text{atm}} \tag{24}$$

In Fig. 4, the calculated values of D_O^T(NiO) have been plotted against $1/T$ together with the results obtained by O'Keeffe and Moore. It can be seen that the magnitude of D_O^T as calculated and as determined experimentally agree satisfactorily. The ratio of D_O^T(CoO) to D_O^T(NiO) thus agrees quite well with that of $[V_O^{\cdot\cdot}]$(CoO) to $[V_O^{\cdot\cdot}]$(NiO). This supports the idea that in both oxides oxygen diffusion occurs via oxygen vacancies.

Because $V_O^{\cdot\cdot}$ is a minority defect over the whole stability range of both CoO and NiO, it is not possible to determine $D_{V_O^{\cdot\cdot}}$ and $[V_O^{\cdot\cdot}]$ separately.

MECHANISM OF OXIDATION

Owing to the difference in oxygen pressure on the two sides of the oxide, concentration gradients arise which cause diffusion to occur. The general equation for the diffusion flux J_{def} is:

$$J_{\text{def}} = -D_{\text{def}}(\partial[\text{def}]/\partial x) \pm \mu_{\text{def}}[\text{def}](\partial\psi/\partial x) \tag{25}$$

where

$$[\text{def}] = [V'_M], [V''_M], [V_O^{\cdot\cdot}], [h^{\cdot}], [e']$$

(note that the + and − signs relate to the effective charges of the defects) and where $\partial\psi/\partial x$ is the potential difference caused by the difference in mobility of defects, D_{def} is the diffusion coefficient of defect, and μ_{def} is the mobility of defect. The diffusion coefficient and defect mobility are related by the Nernst–Einstein equation:

$$D_{\text{def}} = (kT/|ne_0|)\mu_{\text{def}} \tag{26}$$

where $|ne_0|$ is the absolute value of effective charge of defect and e_0 is the charge of electron.

The diffusion is subject to the following general conditions:

(a) The net current must be zero, giving

$$J_{V_M'} + 2J_{V_M''} + J_{e'} = J_{h^\cdot} + 2J_{V_O^{\cdot\cdot}} \tag{27}$$

(b) The total flux must be constant everywhere in the oxide layer:

$$J_{\text{tot}} = J_{V_M'} + J_{V_M''} - J_{V_O^{\cdot\cdot}} = \text{constant} \tag{28}$$

(c) The electroneutrality condition must be satisfied.

Because $\mu_{h^\cdot}$ and $\mu_{e'}$ are much larger than $\mu_{V_M'}$, $\mu_{V_M''}$ and $\mu_{V_O^{\cdot\cdot}}$ it follows from Eqs. (25), (26), and (27) that

$$\partial\psi/\partial x = (kT/|e_0|[h^\cdot]) \times (\partial[h^\cdot]/\partial x) \tag{29}$$

Using the approximation $D_{V_M'} \approx D_{V_M''}$ which has been shown to apply to CoO we find for the total flux:

$$\begin{aligned} J_{\text{tot}} = {} & -2D_{V_M'}\frac{\partial[h^\cdot]}{\partial x} + D_{V_M'} \times K_c\left\{\partial\left(\frac{[h^\cdot]}{2K_c + [h^\cdot]}\right)\Big/\partial x\right\} \\ & + 6D_{V_O^{\cdot\cdot}} \times K_s\frac{\partial(1/[h^\cdot])}{\partial x} - \frac{2D_{V_O^{\cdot\cdot}} \times K_s}{K_c} \times \frac{\partial \ln[h^\cdot]}{\partial x} \end{aligned} \tag{30}$$

When $[h^\cdot]$ is expressed in mole fractions we have

$$-J_{\text{tot}} = d\Delta x/dt \tag{31}$$

where Δx is the thickness of the oxide layer. If this is compared with the parabolic oxidation rate law in differentiated form

$$d\Delta x/dt = k_x/\Delta x \tag{32}$$

we can deduce, after integration of Eq. (30) and combination with (32) that the parabolic rate constant k_x is given by

$$\begin{aligned} k_x = {} & 2D_{V_M''}[h^\cdot]\Big|_{\text{II}}^{\text{I}} - D_{V_M'} \times \frac{K_c[h^\cdot]}{2K_c + [h^\cdot]}\Big|_{\text{II}}^{\text{I}} - 6D_{V_O^{\cdot\cdot}}\frac{1}{[h^\cdot]}\Big|_{\text{II}}^{\text{I}} \\ & + 2D_{V_O^{\cdot\cdot}}\frac{K_s}{K_c}\ln[h^\cdot]\Big|_{\text{II}}^{\text{I}} \end{aligned} \tag{33}$$

where $|_{II}^{I}$ indicates the difference in the value of the indicated function at the oxygen–oxide interface (I) and at the metal–oxide interface (II).

Substituting $J_{tot} = -k_x/\Delta x$ in Eq. (30) leads to

$$\frac{\partial[h^{\cdot}]}{\partial x} = k_x \Big/ \left(\Delta x \left\{ 2D_{V_M^{\cdot}} - \frac{2D_{V_M^{\cdot}} K_c^2}{(2K_c + [h^{\cdot}])^2} + \frac{6D_{V_O^{\cdot\cdot}} K_s}{[h^{\cdot}]^2} + \frac{2D_{V_O^{\cdot\cdot}} K_s}{K_c[h^{\cdot}]} \right\} \right) \tag{34}$$

and after integration we obtain from this:

$$\frac{x}{\Delta x} = \frac{1}{k_x} \left\{ 2D_{V_M^{\cdot}}[h^{\cdot}] - \frac{D_{V_M^{\cdot}} K_c[h^{\cdot}]}{2K_c + [h^{\cdot}]} - \frac{6D_{V_O^{\cdot\cdot}} K_s}{[h^{\cdot}]} + \frac{2D_{V_O^{\cdot\cdot}} K_s}{K_c} \ln[h^{\cdot}] \right\} + C \tag{35}$$

where the integration constant C is calculated from the condition that $x = 0$ at the oxide–metal interface and where $x/\Delta x$ is the relative position in the oxide layer. Thus, from Eqs. (34) and (35) we can calculate $[h^{\cdot}]$ and $\partial[h^{\cdot}]/\partial x$ as $f(x/\Delta x)$ and, using the relationships derived in the section on defect structure, the other defect concentrations and concentration gradients as a function of position in the oxide layer.

Combination of Eq. (25) and Eqs. (1) to (9) finally enables us to calculate the fluxes of the different defects. In this way we obtain the expressions:

$$J_{V_M^{\cdot}} = D_{V_M^{\cdot}} \left\{ -2 + \frac{2K_c}{2K_c + [h^{\cdot}]} + \frac{4K_c^2}{(2K_c + [h^{\cdot}])^2} \right\} \frac{\partial[h^{\cdot}]}{\partial x} \tag{36a}$$

$$J_{V_M^{''}} = D_{V_M^{\cdot}} \left\{ -\frac{2K_c^2}{(2K_c + [h^{\cdot}])^2} - \frac{2K_c}{2K_c + [h^{\cdot}]} \right\} \frac{\partial[h^{\cdot}]}{\partial x} \tag{36b}$$

$$J_{V_O^{\cdot\cdot}} = D_{V_O^{\cdot\cdot}} K_s \left\{ \frac{6}{[h^{\cdot}]^2} + \frac{2K}{K_c[h^{\cdot}]} \right\} \frac{\partial[h^{\cdot}]}{\partial x} \tag{36c}$$

Because $[h^{\cdot}]$ and $\partial[h^{\cdot}]/\partial x$ can be defined as functions of $(x/\Delta x)$ it is also possible for the fluxes to be expressed in this way. In the last equation we have used the vacancy diffusion coefficient of oxygen which can be shown to be related to the tracer diffusion coefficient of oxygen by

$$D_{V_O^{\cdot\cdot}} \times K_s = (D_O^T/f) \times K_c \tag{37}$$

where f is the correlation factor.

CALCULATION OF OXIDATION RATES AND DIFFUSION FLUXES

Using the numerical data from pages 186–193 and Eq. (33), the oxidation rate of Co is found to be given by

$$k_{x,Co} = 50.8 \times 10^{-3} \times \exp(-33{,}600/RT) \times p_{O_2}^{1/4} \tag{38}$$

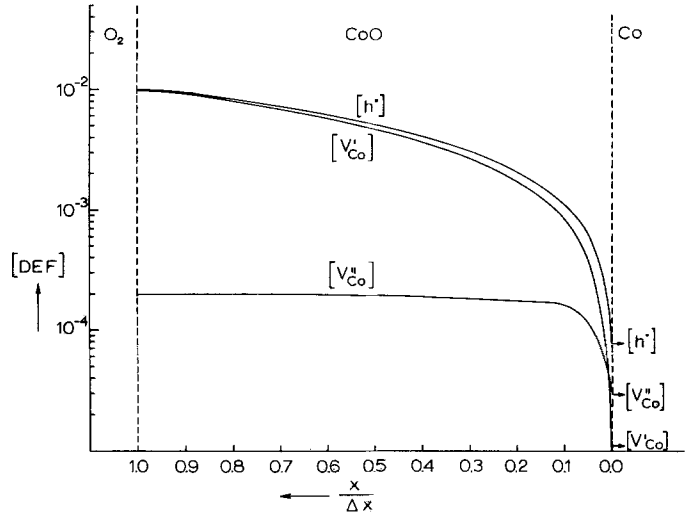

Fig. 5. Defect concentrations in CoO during oxidation of Co at $p_{O_2} = 1$ atm and $t = 1146°C$.

when $D_{V'_{Co}}$ is taken to be independent of p_{O_2}. Because this is not quite true (since $D_{V'_{Co}}$ decreases somewhat with increasing p_{O_2}), we have $k_{x,Co} \sim p_{O_2}^{1/n}$ with n slightly smaller than 4.

From the experimental results of Carter and Richardson[18] and of Bridges *et al.*[19] it can be calculated that

$$k_{x,Co}(\text{exp}) = 4.3 \times 10^{-3} \times \exp(-34{,}000/RT) \times p_{O_2}^{1/3,3} \tag{39}$$

The calculated rate constant [Eq. (38)] thus shows good agreement with this experimental result.

In Fig. 5 $[h^{\cdot}]$, $[V'_{Co}]$, and $[V''_{Co}]$ are plotted as functions of position in the oxide layer during oxidation of Co at 1146°C and $p_{O_2} = 1$ atm. The electron hole concentration $[h^{\cdot}]$ was calculated from Eq. (35) and the corresponding values of $[V'_{Co}]$ and $[V''_{Co}]$ were then derived using the values of $K_a K_b$ and K_c. It is seen that over 90% of the oxide layer thickness $[V'_{Co}]$ closely approximates to $[h^{\cdot}]$. Also it can be seen that $[V''_{Co}]$ is constant over the greater part of the oxide layer and only starts to decrease appreciably, although at a slower rate than $[V'_{Co}]$, in the vicinity of the metal–oxide interface. The concentration $[V''_{O}]$ is not given in Fig. 5 because (as was discussed earlier) its absolute value cannot be determined; it is only possible to state that $[V''_{O}] \sim 1/[V''_{Co}]$.

Using Eqs. (36a–c) together with the appropriate numerical results of the second and third sections, the contributions of the different defects to the

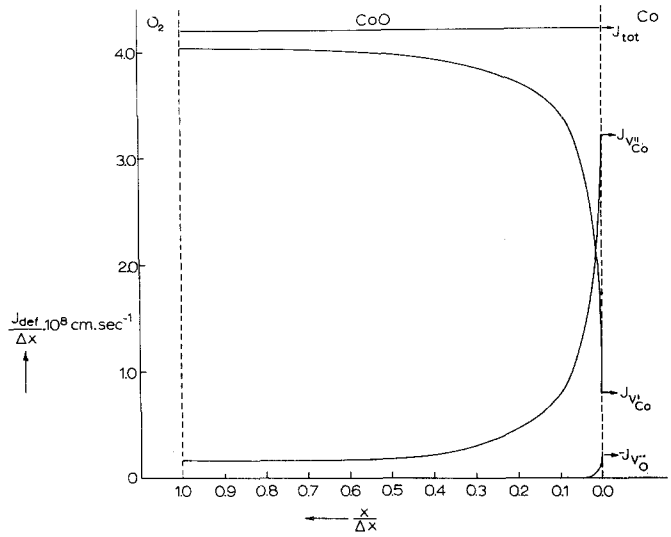

Fig. 6. Diffusion fluxes in CoO during oxidation of Co at $p_{O_2} = 1$ atm and $t = 1146°C$.

oxidation were calculated; these are shown in Fig. 6. On the gas side, diffusion of mononegative Co vacancies is seen to be mainly responsible for transport, while on the metal side a significant contribution of dinegative vacancies is to be noted. The contribution of oxygen diffusion remains smaller than 3% of the total at all positions in the layer. Very similar results are obtained from calculations at other temperatures between 950 and 1350°C.

In the same way the oxidation rate constant of Ni was calculated from the results of the second and third sections and is given in Fig. 7. The upper line (a) was calculated with, and the lower (b) without the contribution of oxygen vacancies to the transport through the oxide layer. We see that, depending upon the temperature, oxygen transport causes an increase of between 15 and 40% in the calculated rate constant.

Sartell and Li,[20] Frederick and Cornet,[21] and Philips[22] have determined the oxidation rate of very pure Ni (total amount of impurities < 20 ppm) in air. From their experimental results $k_{x,Ni}$ (exp) has also been calculated at $p_{O_2} = 1$ atm (using the assumption that $k_{x,Ni} \sim p_{O_2}^{1/5}$) and given in Fig. 7. There is a reasonable agreement between the calculated and experimental values. Owing to the scatter in the experimental results, it is impossible, however, to conclude from these data whether oxygen diffusion indeed contributes to the oxidation rate of Ni. In the next section we shall return to this question.

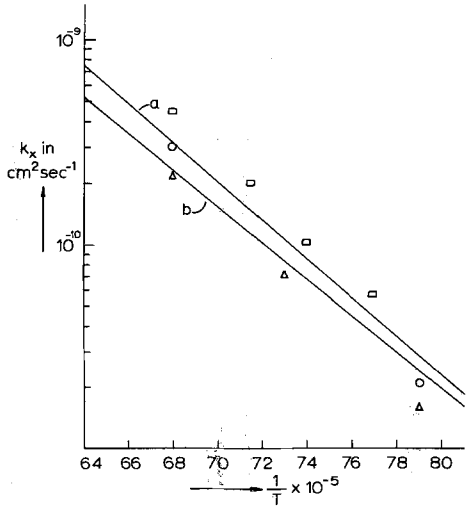

Fig. 7. Calculated and experimental values of the oxidation rate constant k_x of Ni as a function of temperature at $p_{O_2} = 1$ atm. □, Ref. 20; ○, Ref. 21; △, Ref. 22. a, Calculated with $D_O^T = 1.5 \times 10^{12}$, *bij* $p_{O_2} = 0.065$ atm; b, calculated with $D_O^T = 0$.

In Fig. 8 the defect concentrations in NiO, calculated in the same way as for CoO, are shown as a function of position in the oxide layer. From this figure we deduce that during oxidation of nickel V'_{Ni} is the majority defect close to the oxide–gas interface, while V''_{Ni} is the predominant defect close to the oxide–metal interface. Here again it is impossible to calculate the absolute value of $[V_O^{\cdot\cdot}]$. The contributions of the different fluxes to the total transport in NiO were calculated using Eqs. (36a–c) and are seen in Fig. 9.

Near the oxide–gas interface, diffusion occurs mainly via mononegative metal ion vacancies. Nearer to the metal–oxide interface we see an increased contribution to diffusion from dinegative metal ion vacancies. At the same time, however, $J_{V_O^{\cdot\cdot}}$ also increases. This causes $J_{V''_{Ni}}$ to pass through a maximum. At the metal–oxide interface itself the transport is mainly due to oxygen vacancies.

MARKER EXPERIMENTS

Both spectrochemically pure Co and Ni have been oxidized using platinum as a marker. As is shown in Fig. 10, the marker is found in the cobalt–oxide layer on the interface between a relatively fine-grained, porous inner layer and a thick, coarse-grained outer layer. At lower oxygen pressures,

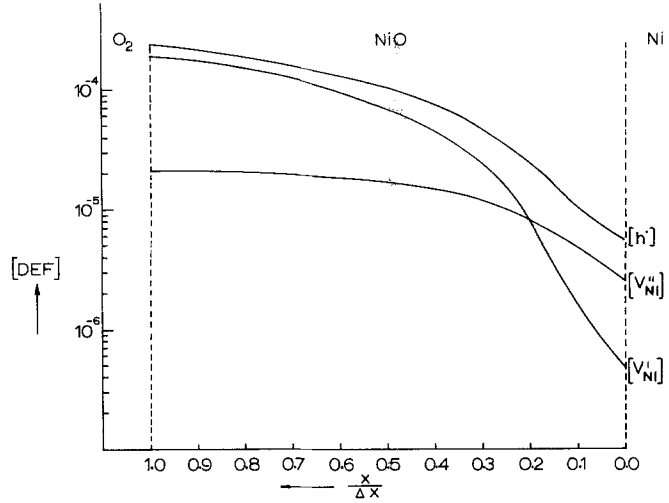

Fig. 8. Defect concentrations in NiO during oxidation of Ni at $p_{O_2} = 1$ atm and $t = 1166°C$.

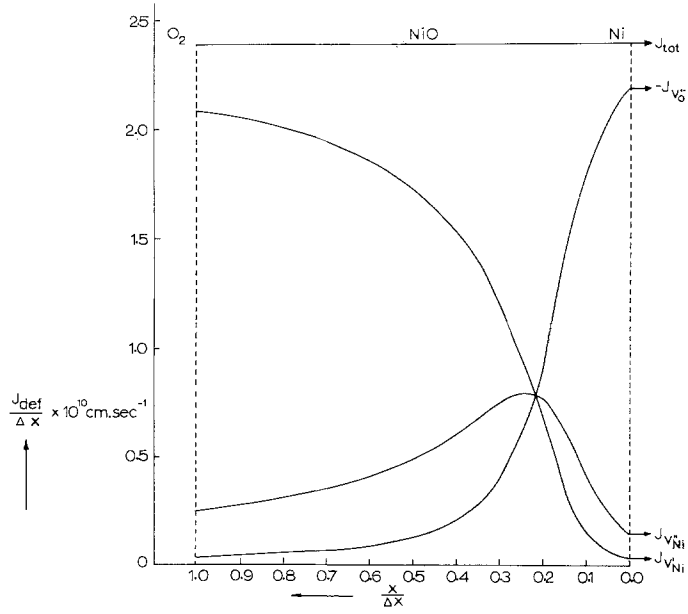

Fig. 9. Diffusion fluxes in NiO during oxidation of Ni at $p_{O_2} = 1$ atm and $t = 1166°C$.

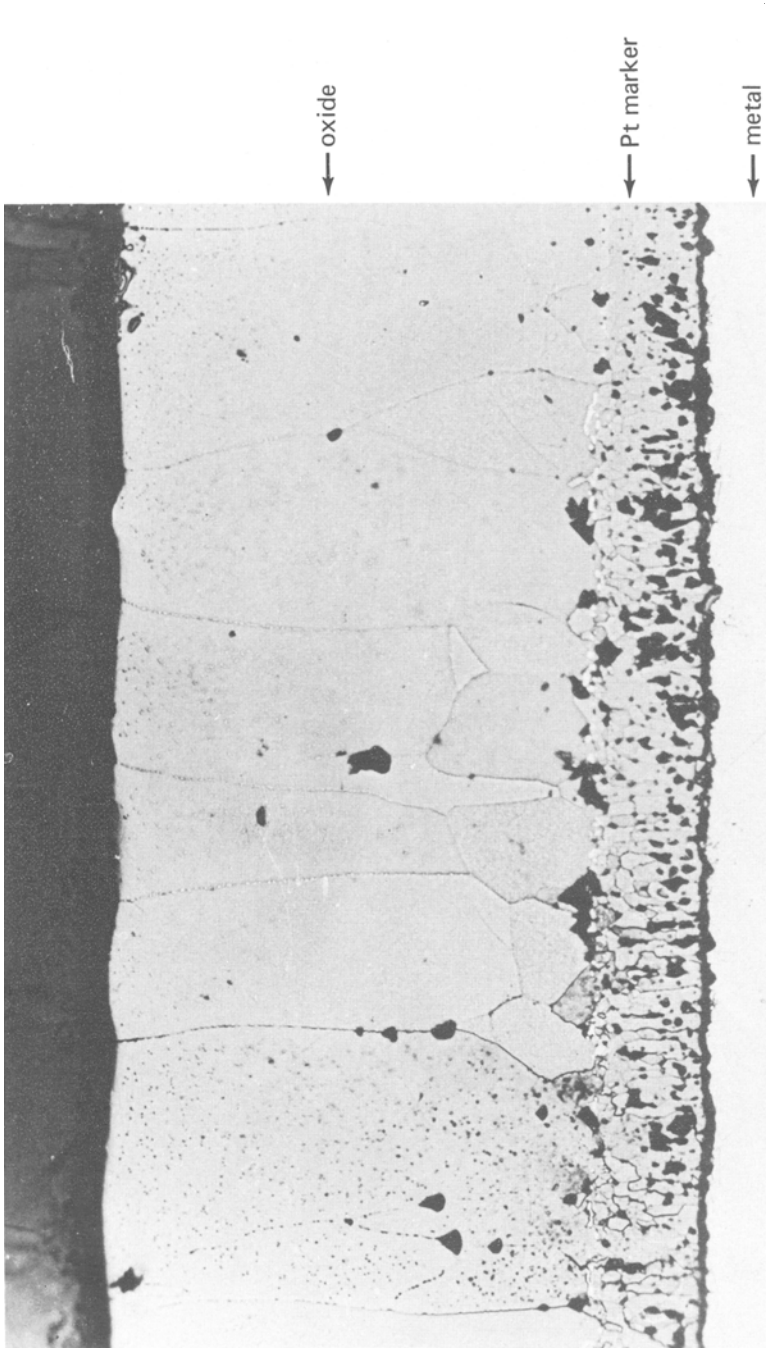

Fig. 10. Co oxidized in air for 3 hr at 1050°C. × 180, reduced 10% for reproduction.

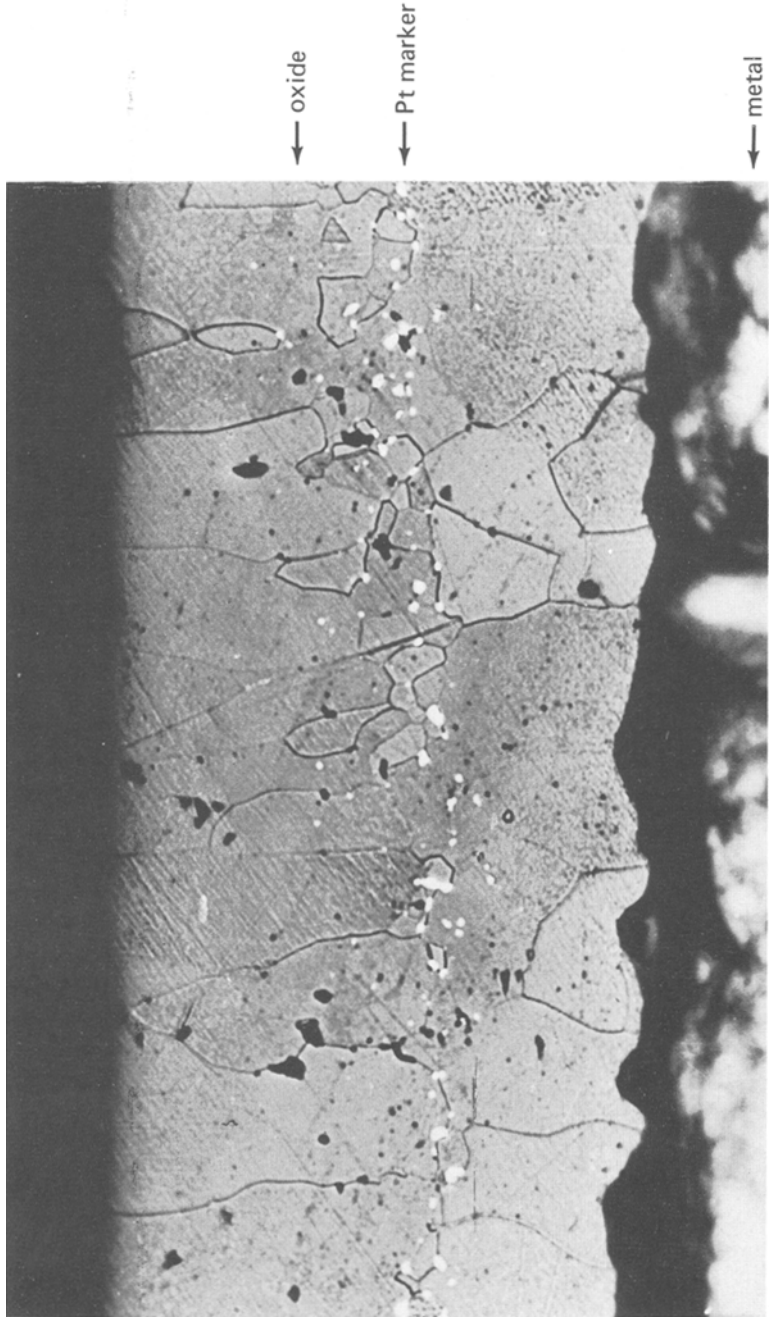

Fig. 11. Ni oxidized in air for 80 hr at 1250°C. Note the separation between metal and oxide occurred during micro preparation. × 260, reduced 10% for reproduction.

i.e., at a lower oxidation rate, the thickness of this inner layer decreases from about 16% to about 4% of the total thickness when p_{O_2} is changed from 1 atm to 5×10^{-3} atm. This is in agreement with the theory proposed by Mrowec and Werber[23] for the formation of porous inner layers in the oxidation of metals where only cation diffusion occurs. If, according to these authors, the oxidation rate is high enough, pores are formed owing to the accumulation of vacancies when they are not annihilated rapidly enough by plastic deformation. The Pt marker then loses contact with the metal and becomes embedded within the oxide on top of the porous inner layer.

In the case of Ni, a nonporous NiO layer is formed as seen in Fig. 11. Because Ni oxidizes much more slowly than Co($k_{x,Ni} \sim 0.01 k_{x,Co}$) plastic deformation is fast enough in this case to prevent the formation of pores. Nevertheless, the marker is found nearly in the middle of the otherwise homogeneous oxide layer.

This is just what is expected from the model presented above, where oxygen diffusion occurs near the metal–oxide interface and cation diffusion at the gas–oxide interface. The fact that changes in oxygen pressure or temperature do not significantly influence the position of the marker in this case also supports this model.

SUMMARY AND CONCLUSIONS

Starting from a general model for the defect structure of nickel and cobalt oxides, the concentrations and diffusion coefficients of the majority defects in these oxides have been determined as a function of temperature and oxygen pressure. This led to the conclusion that it is highly probable that the anion defects are dipositive oxygen vacancies. These are minority defects, however, so that their concentrations and diffusion coefficients could not be determined separately. At the higher oxygen pressures the predominant cation defects are mononegative metal ion vacancies, while at lower oxygen pressures appreciable concentrations of dinegative metal ion vacancies are present.

Upon the basis of this defect structure, a model for the oxidation of Co and Ni was proposed. When the conclusions from this model were compared with experimental results, good agreement was observed. In this way it has been shown that probably more than one type of defect contributes to the total transport through the oxide. For cobalt these are mono- and dinegative metal ion vacancies, while for nickel, dipositive oxygen vacancies also make a significant contribution.

ACKNOWLEDGMENT

The authors would like to thank all those who contributed to this work, in particular M. A. de Jonghing for his help in the microscopic investigation and A. van der Scheer, B.t.w. for the calculations of defect concentrations.

REFERENCES

1. C. Wagner, *Z. Physik. Chem.* **21**, 25 (1935).
2. C. Wagner, *Z. Physik. Chem.* **32**, 447 (1936).
3. F. A. Kröger, *The Chemistry of Imperfect Crystals* (North Holland, Amsterdam, 1964).
4. W. van Gool, *Principles of Defect Chemistry of Crystalline Solids* (Academic Press, New York and London, 1966).
5. N. G. Eror and J. B. Wagner, *J. Phys. Chem. Solids* **29**, 1597 (1968).
6. B. Fischer and D. S. Tannhauser, *J. Chem. Phys.* **44**, 1663 (1966).
7. G. H. Meyer and R. A. Rapp, *Z. Physik. Chem. N.F.* **74**, 168 (1971).
8. W. Jost, *Diffusion* (Academic Press, New York, 1960).
9. J. Crank, *Mathematics of Diffusion* (Clarendon Press, Oxford, 1957).
10. J. B. Price and J. B. Wagner, *Z. Physik. Chem. N.E.* **49**, 257 (1966).
11. W. K. Cheng, N. L. Peterson, and W. T. Reeves, *Phys. Rev.* **186**, 887 (1969).
12. R. E. Carter and F. D. Richardson, *Trans. AIME* **200**, 1244 (1954).
13. W. K. Chen and R. A. Jackson, *J. Phys. Chem. Solids* **30**, 1309 (1969).
14. J. B. Holt, *Proc. Br. Ceram. Soc.* **9**, 157 (1967).
15. B. A. Thompson, Ph.D. Thesis, Rensselaer Polytechnic Institute, 1962.
16. M. O'Keeffe and W. J. Moore, *J. Phys. Chem.* **65**, 1438, 2277 (1961).
17. P. Reynen, in: Reactivity of Solids, *Proc. 6th Intern. Symp.* (Schenectady, New York, 1968), p. 99.
18. R. E. Carter and F. D. Richardson, *Trans. AIME* **203**, 336 (1955).
19. D. W. Bridges, J. P. Baur, and W. M. Fassel, *J. Electrochem. Soc.* **103**, 619 (1956).
20. J. A. Sartell and C. H. Li, *J. Inst. Metals* **90**, 62 (1961).
21. S. F. Frederick and J. Cornet, *J. Electrochem. Soc.* **102**, 285 (1955).
22. W. L. Philips, *J. Electrochem. Soc.* **110**, 1014 (1963).
23. S. Mrowec and T. Werber, *Acta Met.* **8**, 819 (1960).